

A 250 MHz low voltage low-pass G_m -C filter

Tien-Yu Lo · Chung-Chih Hung

Received: 13 October 2010 / Revised: 5 March 2011 / Accepted: 27 May 2011 / Published online: 11 June 2011
© Springer Science+Business Media, LLC 2011

Abstract A high speed and high linearity G_m -C low-pass filter is presented. The proposed OTA is designed under low power supply voltage consideration while its gain, excess phase, and linearity are well maintained. The common-mode control system, including common-mode feedback and common-mode feedforward circuits, is added to ensure stability of the proposed filter. Measurement results show that the inter-modulation distortion of -40 dB can be achieved with 250 MHz 400 mV_{pp} balanced differential input signals. The filter works in 1 – V supply voltage and its power consumption is 32 mW.

Keywords Operational transconductance amplifier (OTA) · Filter · Ultra-wide band system

1 Introduction

As there is a great demand for lighter hand-held mobile phones and longer battery lifetime, low-voltage integrated circuit design solutions must be developed. Traditionally in CMOS technology, the baseband filters are realized with switched-capacitor (SC) techniques, but the SC filters are limited to low speed applications due to the sampling procedure and the high power requirement of the OPAMP. On the other hand, continuous-time G_m -C filter realizations can be easily implemented for the high speed applications

and tend to be less power consuming. Furthermore, the filters do not require extra processing steps compared with Active-RC structures, and their frequency tuning can be easily achieved. Thus, the G_m -C filter appears to be a better candidate for the UWB wireless application, which uses pulse signals at a high speed.

For G_m -C filter implementation, the high performance operational transconductance amplifier (OTA) would be the most important building block [1–4]. In the design of OTAs, the transconductance should be tuned for compensation for process tolerances and temperature variations without degrading the entire circuit performance. Besides, low power supply voltage implementation should be adopted for the trend of a system-on-a-chip strategy. The performance of digital circuits does not degrade when using lower power supply voltage. On the other hand, for analog circuits, the circuit performance is strongly affected by the low power supply voltage. The linearity performance of the OTA will become worse at low supply voltage, so novel OTA circuit design should be investigated.

In this article, the design of a high speed, low distortion and low supply voltage G_m -C filter for UWB wireless application is presented. The structure of the high linearity OTA with the pseudo-differential pair is discussed in Sect. 2. The common-mode control system with guaranteed stability is shown in Sect. 3. In Sect. 4, the design of fourth-order equiripple linear phase low-pass filter and the measurement results are discussed. Some final conclusions are presented in Sect. 5.

2 Proposed OTA

To design a high performance OTA, the concept of voltage attenuation is taken in our circuit. Figure 1 shows the block

T.-Y. Lo · C.-C. Hung (✉)
Analog Integrated Circuit Laboratory, Department of Electrical Engineering, National Chiao Tung University, Hsinchu 300, Taiwan, ROC
e-mail: cchung@mail.nctu.edu.tw

T.-Y. Lo
e-mail: tienyu.lo@gmail.com

diagram of the technique. The factor ζ is smaller than 1. We can see that the input voltage is attenuated by the value ζ and the output current is given by

$$i_o = a_1(\zeta v_i) + a_2(\zeta v_i)^2 + a_3(\zeta v_i)^3 \tag{1}$$

We can prove that the third-order harmonic distortion term (HD3) gets a value of ζ^2 smaller than the original one. The natural attenuation could be obtained from the designed capacitor ratio, and thus the multiple input floating-gate (MIFG) technique can be a good approach [5, 6]. However, large capacitors limit the operation speed and technique requires extra fabrication processes. In this article, the high speed OTA, which operates under the concept of voltage attenuation to achieve high linearity in standard CMOS process, is presented.

A pseudo-differential structure [7–9] is also used in our circuit for low voltage operation. The absence of the tail current source allows lower power supply voltage and higher signal swing ranges. For large device length, the pseudo-differential pair with the source terminals connected to ground obtains more linear performance in contrast with the fully-differential architecture. However, in the technology down to smaller feature sizes, the short channel effect occurs owing to the fact that the effective carrier mobility is a function of both the longitudinal and transversal electric fields, and thus the short channel effect and channel length modulation will degrade the linearity of the pseudo-differential structure.

Figure 2 shows the proposed OTA circuit. Resistor R_{tune} is connected between current mirrors M3 and M4. By using the resistor, we can obtain a voltage attenuation factor of $\zeta = g_{m(1,2)} \times R_{tune} / (2 + g_{m(3,4)} \times R_{tune})$ from the gate terminal to the drain terminal of transistors M1 and M2, where $1/g_{m(3,4)}$ is the output impedance of diode-connected transistors. If we have a small value of $g_{m(3,4)} \times R_{tune}$, a high attenuation factor can be achieved. In order to obtain the linearity performance, we adopt the usual mobility equation $\mu_{n,p} = \mu_0 / (1 + \theta V_{ov})$, where μ_0 is low-field mobility, θ is the mobility reduction coefficient, and V_{ov} is the MOS over-drive voltage. By taking the output current equation into a Taylor series expansion, the third-order harmonic distortion component of the OTA is given by

$$HD_3 \cong \frac{\theta}{16V_{ov(1,2)} \left(1 + \theta V_{ov(1,2)} \sqrt{\frac{BK(3,4)}{K(1,2)}}\right)^2 \left(2 + \theta V_{ov(1,2)} \sqrt{\frac{BK(3,4)}{K(1,2)}}\right) \sqrt{\frac{K(1,2)}{BK(3,4)}} \left(\frac{K(1,2)}{K(3,4)} \zeta V_p\right)^2} \tag{2}$$

where K_i is the device parameter of transistor M_i , V_p is the peak voltage of a sinusoid input signal, and B is the current mirror ratio of M3–M5 and M4–M6.

The gain performance of the OTA should be maintained as well. Usually, the gain of larger than 30 dB is sufficient for low Q low-pass filter design for correct signal transformation [10], and it could be maintained by designing a small aspect ratio of load transistors. Unfortunately, the use of R_{tune} would highly degrade the overall gain. Cascode circuit could be a possible solution, but it would not suitable for the low voltage design.

By taking the gain performance into consideration, the modified OTA circuit is shown in Fig. 3. Transistor M11 has the same size as transistors M1 and M2, and thus it has the same drain current by giving the same input common-mode voltage at the gate terminal. Transistors M9 and M10, which work in the saturation region with α times aspect ratio with respect to M12, are utilized to share part of DC drain current from M1 and M2. The increased gain would be expressed as

$$A_{enhanced} = \left(\frac{2\sqrt{(1-\alpha)} + g_{m(3,4)}R_{tune}}{2 + g_{m(3,4)}R_{tune}} \right) \left(\frac{1}{1-\alpha} \right) \tag{3}$$

For example, if the value of α is 3/4, we can obtain that $1 - \alpha$ would be equal to 1/4, and thus an enhanced gain in the range of 2–4 can be achieved. We should note that the

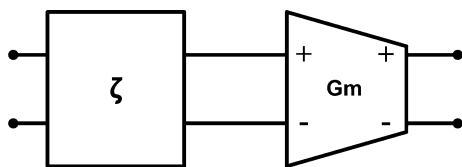


Fig. 1 Concept of voltage attenuation

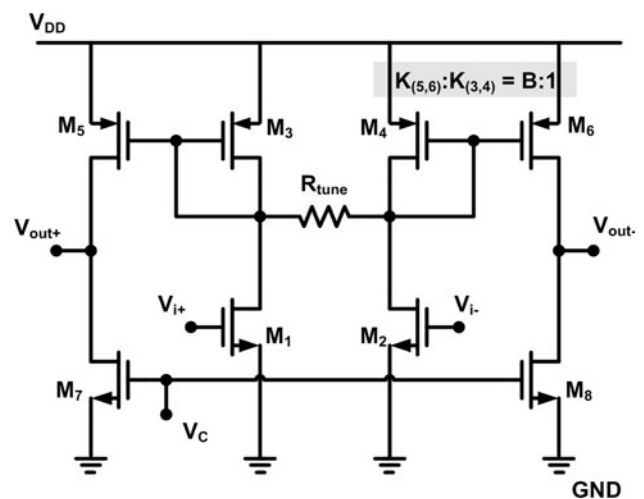


Fig. 2 Linearized low voltage OTA circuit

structure also increases the linearity performance because the value of $gm_{(3,4)}$ in Fig. 3 has a factor of $\sqrt{(1-\alpha)}$ then the value of $gm_{(3,4)}$ in Fig. 2, and thus a smaller value of ζ can be obtained. In other words, it could relax the required sizes of transistors M3 and M4, and the value of R_{tune} . Moreover, transistors M9 and M10 would not affect the linearity performance owing to their high output impedance. Therefore, the OTA gain could be expressed as where C_X and C_L are the capacitance at nodes $V_{X(a,b)}$ and

output voltage, but suppresses input common-mode signal at the output stage. For the fully-differential structure, the common-mode feedback (CMFB) circuit is used as a negative feedback loop that fixes the output common-mode voltage. The tail current source in the fully-differential structure would restrict the input common-mode signal from variation. For the pseudo-differential structure, the way of suppressing the input common-mode signal is to include a common-mode feedforward (CMFF) circuit.

$$A(s) = \sqrt{\frac{K_{(1,2)}K_{(3,4)}}{1-\alpha}} \left(\frac{R_{tune}}{2 + \sqrt{K_{(1,2)}K_{(3,4)}(1-\alpha)}V_{ov(1,2)}R_{tune}} \right) \frac{1}{\lambda_{(5,6)} \left(1 + s \frac{C_L}{2\lambda_{(5,6)}B(1-\alpha)K_{(1,2)}V_{ov(1,2)}^2} \right)} \frac{1}{\left(1 + s \frac{R_{tune}C_X}{2 + \sqrt{K_{(1,2)}K_{(3,4)}(1-\alpha)}V_{ov(1,2)}R_{tune}} \right)} \tag{4}$$

$V_{out(+/-)}$, respectively. The term λ accounts for the effect of channel length modulation. The non-dominant pole should be carefully designed for smaller excess phase so that the OTA can connect load capacitance C_L at the output to implement an integrator. The higher excess phase of the OTA will cause deviation to the -3 dB cutoff frequency of the resulting filter. We can see from (3) that the non-dominant pole would be affected by the value of α so as to contribute excess phase. Thus, the tradeoff among stability, gain, and linearity should be considered simultaneously.

3 The common-mode control system

The differential-output OTA requires proper common-mode control which not only stabilizes DC common-mode

Figure 4 illustrates an efficient common-mode control system, which is implemented by the CMFF circuit combined with the CMFB circuit. The CMFF circuit is composed by transistors MFFP1, MFFP2, and MFFN. The resistor R_{tune} is replaced by two MOS transistors operating in the linear region, and thus the output common-mode voltage can be simply sensed by next OTA in the cascaded biquadratic structure. The value of R_{tune} is equal to $1/(K_{(r1)} \times V_{ov(r1)}) + 1/(K_{(r2)} \times V_{ov(r2)})$, where $V_{ov(r1,r2)}$ is equal to $V_{tune} - V_{X(a,b)} - V_t$ and depends on V_{tune} . We should design the transistor sizes that $K_{(5,6)} = K_{(FFP1,FFP2)}$, $2 \times K_{(7,8)} = K_{(FFN)}$, $K_{(1,2)} = K_{(FBN)}$, and $K_{(3,4)} = K_{(FBP)}$. In the figure, the CMFB loop is drawn in bold lines.

The CMFB circuit senses the output common-mode voltage from next OTA and produces corrected current to the CMFF circuit. Like in the previous discussion, the

Fig. 3 Modified low voltage OTA circuit

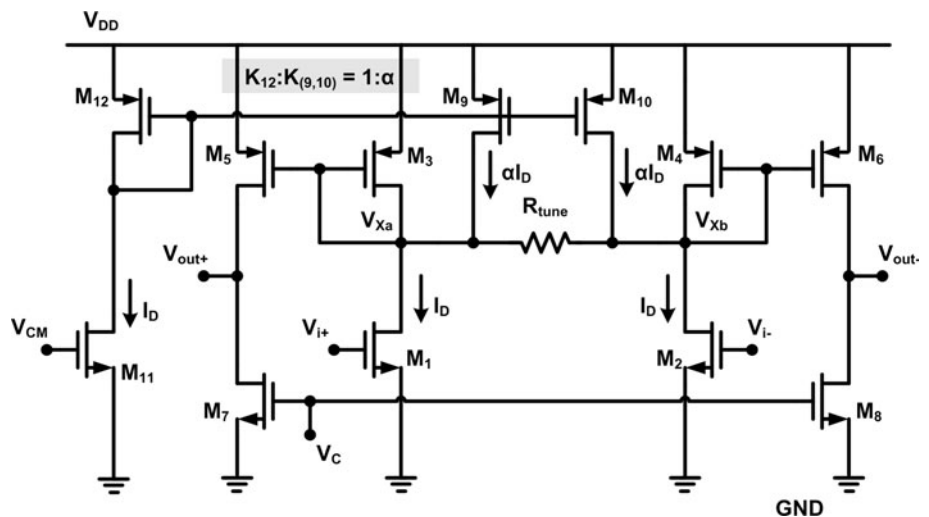
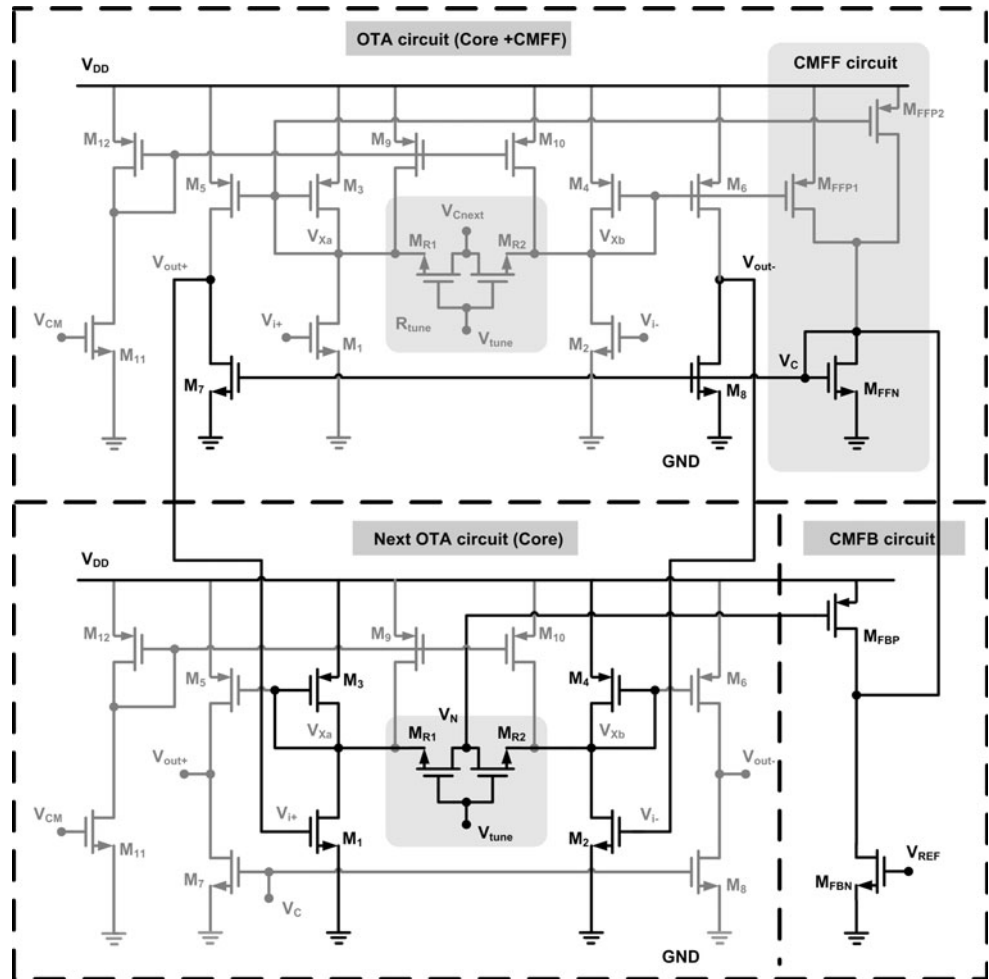


Fig. 4 The common-mode control system



common-mode control system is also designed under the consideration of high speed with stable phase margin. The open loop gain of the CMFB circuit is given by

$$A_{CMFB}(s) \approx g_{CMFB}(s) \frac{1}{(g_{o5,6} + g_{o7,8})} = \frac{g_{m(1,2)}}{(g_{o5,6} + g_{o7,8})} \frac{1}{(1 + s \frac{R_{tune} C_N}{2}) (1 + s \frac{C_C}{g_{mFFN}}) (1 + s \frac{C_L}{g_{o5,6} + g_{o7,8}})} \tag{5}$$

where C_C and C_N is the capacitance at nodes V_C and V_N , respectively. Again, the modified structure increases the gain of the CMFB as well. The dominant pole of the circuit is $(g_{o5,6} + g_{o7,8})/C_L$ and the non-dominant high frequency poles are at g_{mFFN}/C_C and $2/R_{tune} \times C_N$. It is necessary to ensure that the frequency of the non-dominant poles would be larger than the unity-gain bandwidth.

The CMFF circuit uses replica current mirror of M5 and M6. It senses the input common-mode signal from two terminals of the resistor and cancels the common-mode signal variation. For the common-mode control operation, the error value will be sent from the CMFB part as an

adaptive bias signal and combined with the CMFF part for overall stability. The input common-mode gain in our design can be also calculated as

$$A_{cm}(s) \approx \frac{(g_{o5,6} + g_{o7,8})}{g_{CMFF}(s) + g_{CMFB}(s)} \text{ where } g_{CMFF}(s) = Bg_{m(1,2)} \times \frac{1}{(1 + s \frac{BR_{tune} C_N}{2}) (1 + s \frac{C_C}{g_{mFFN}}) (1 + s \frac{C_L}{g_{o5,6} + g_{o7,8}})} \tag{6}$$

The result of smaller than one can be obtained at low frequency owing to the large values of g_{CMFB} and g_{CMFF} , and thus a higher CMRR can be expected.

4 Filter implementation and measurement results

In the integrator design, the unity-gain frequency would be an important factor for future filter synthesis. The unity-gain frequency is dependent on the transconductance and the loading capacitor. Adjustable transconductor or capacitor is

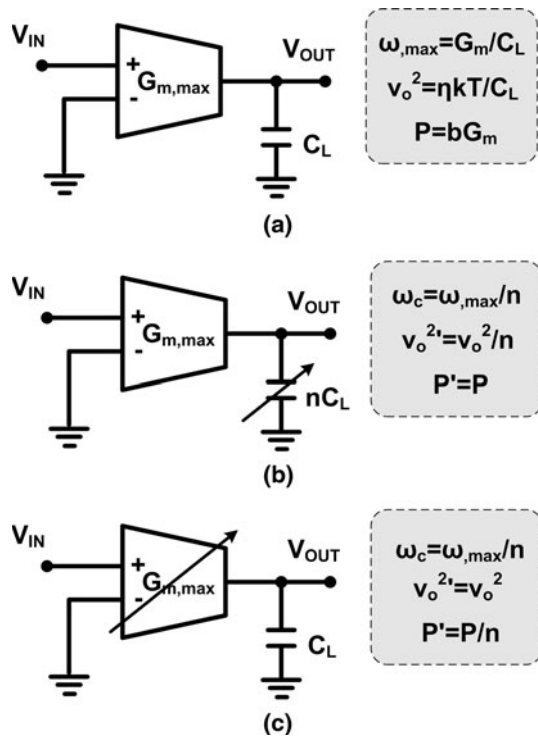


Fig. 5 Integrators: **a** integrator with maximum unity-gain frequency, **b** integrator with constant-Gm design, **c** integrator with constant-CL design

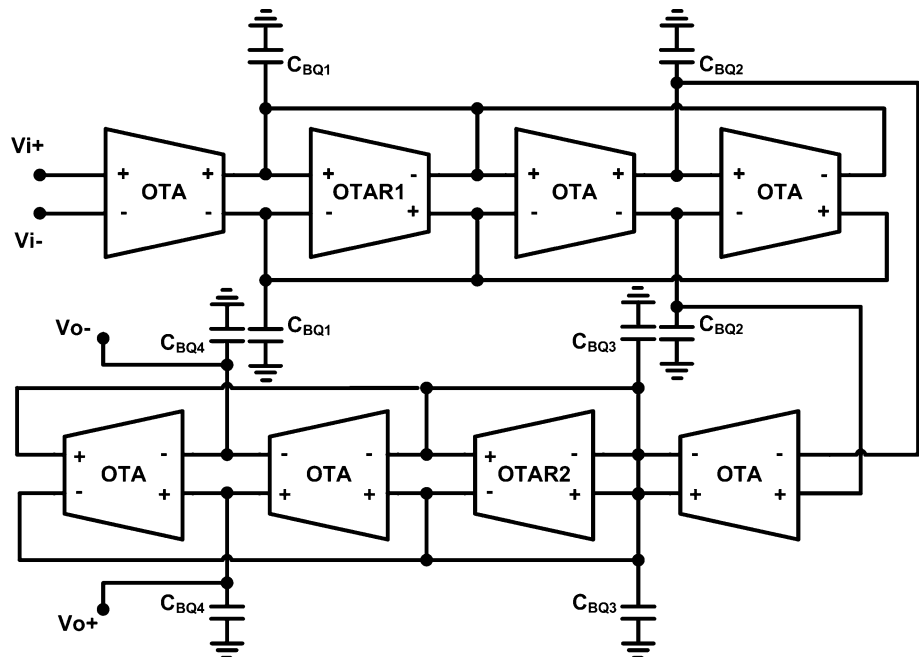
required to compensate process corner variation. Thus, we can keep transconductance constant and vary the capacitance or vice versa. These approaches are called constant-G_m and constant-C_L, respectively. For these approaches, the performance of noise, area, and power dissipation is different.

Figure 5 shows the implementation of the programmable integrator. In Fig. 5(a), the unity-gain frequency is defined by the largest transconductance. The output noise current power spectral density v_o^2 is defined to be $4kT\eta G_m$, where η is the excess noise factor of the transconductor. The power dissipation is assumed to be proportional to the transconductance with a factor b . For a given v_o^2 , the value of C_L is defined and then we obtain a largest value, ω_{max} , through the largest transconductance.

Figure 5(b) and (c) shows the corresponding value when the unity-gain frequency is adjusted. Thus, the noise, capacitor area, and the power will vary accordingly. For the constant-G_m design, a large capacitor area is required and it is not suitable for high frequency applications. The low noise performance is not very helpful since only the highest noise contribution is needed to be defined over the frequency tuning range. In contrast, the constant-C_L design decreases the transconductance, which implies lower power consumption. The noise performance is equal throughout the frequency tuning range without any over-design. Therefore, the constant-C_L approach is preferred in our filter design.

In this article, the fourth-order Gm-C low-pass filter based on the biquadratic section is designed. The requirement of the equiripple linear phase fashion is due to the high speed pulse signal in UWB wireless application to reduce inter-symbol interference (ISI) effect. The implementation of the OTA building block is shown in Fig. 6. The proposed OTA circuit is used for all of the transconductor cells. The number of the CMFB circuits is reduced due to the shared low impedance nodes of lossy integrators.

Fig. 6 The fourth-order equiripple linear phase filter



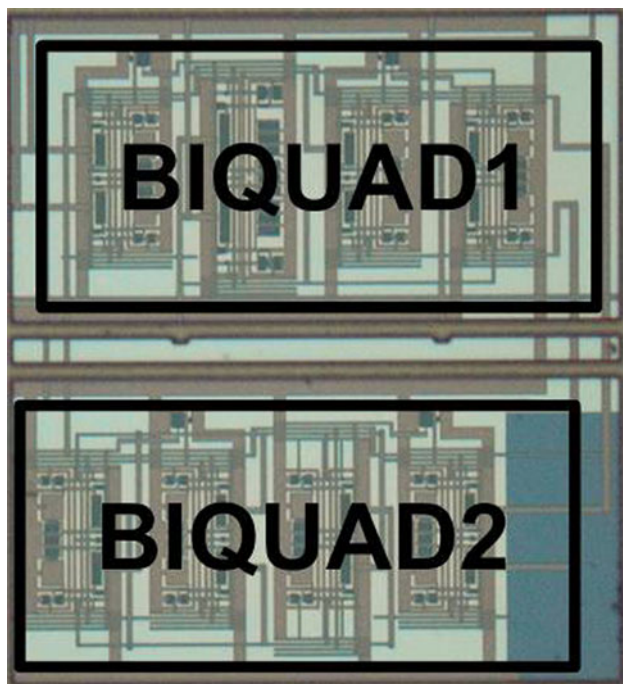


Fig. 7 Die micrograph

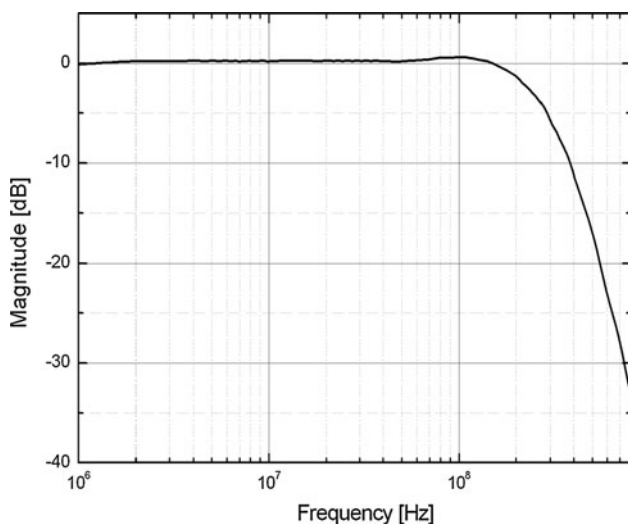


Fig. 8 Measured frequency response of the fourth-order Gm-C filter

The tuning strategy can be achieved by changing the voltage V_{tune} through the use of the MOS transistor operating in the linear region, and the maximum tuning voltage range of $V_{ov}(1,2) \times \sqrt{[(1 - \alpha)K(1,2)/K(3,4)]}$ can be obtained.

The G_m -C filter is designed by using TSMC 0.18- μm CMOS process. The die photograph is shown in Fig. 7, where the active area is $2.4 \times 10^{-2} \text{ mm}^2$. Parasitic capacitances and metal resistances are extracted to simulate

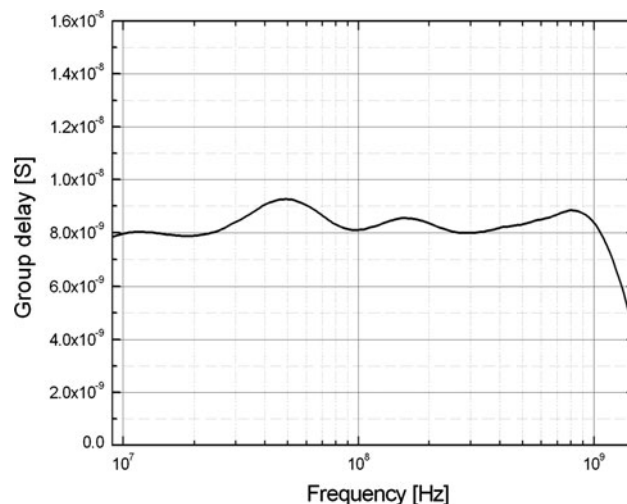


Fig. 9 Measured group delay response of the fourth-order Gm-C filter

the realistic environment. The OTA circuit is simulated by connecting 1 pF capacitance at the output to work as an integrator. The gain of the OTA is nearly 30 dB with 89° phase margin, and the unity-gain frequency is 230 MHz. The current mirror factor α is chosen to be 20/21 and the current mirror ratio B is set to nearly 2. Figure 8 shows the measured magnitude response of the filter. The magnitude response is normalized owing to attenuation from the output buffer. The -3 dB cutoff frequency (f_c) of the low-pass G_m -C filter is 250 MHz and the low frequency CMRR is 35 dB. The group delay is almost constant over f_c and the group delay ripple is less than 2 ns over the range up to f_c , as shown in Fig. 9. The third-order inter-modulation (IM3) distortion with two sinusoidal tones of 400 mV_{pp} is shown in Fig. 10. The IM3 is shown to be less than -40 dB at the speed of 250 MHz.

5 Conclusions

A G_m -C filter implementation with an enhanced-linearity CMOS OTA has been presented, and the design is targeted for UWB wireless application. For the entire filter, the common-mode voltage of the pseudo-differential topology can be well defined by employing suitable CMFB and CMFF circuits. The circuit was fabricated by the TSMC 0.18- μm CMOS process in 1-V power supply voltage with power consumption of 32 mW. Measurement results show that high speed and excellent linearity can be achieved. Table 1 summarizes the performance of this work with recently reported filters.

Fig. 10 Measured two tone inter-modulation distortion

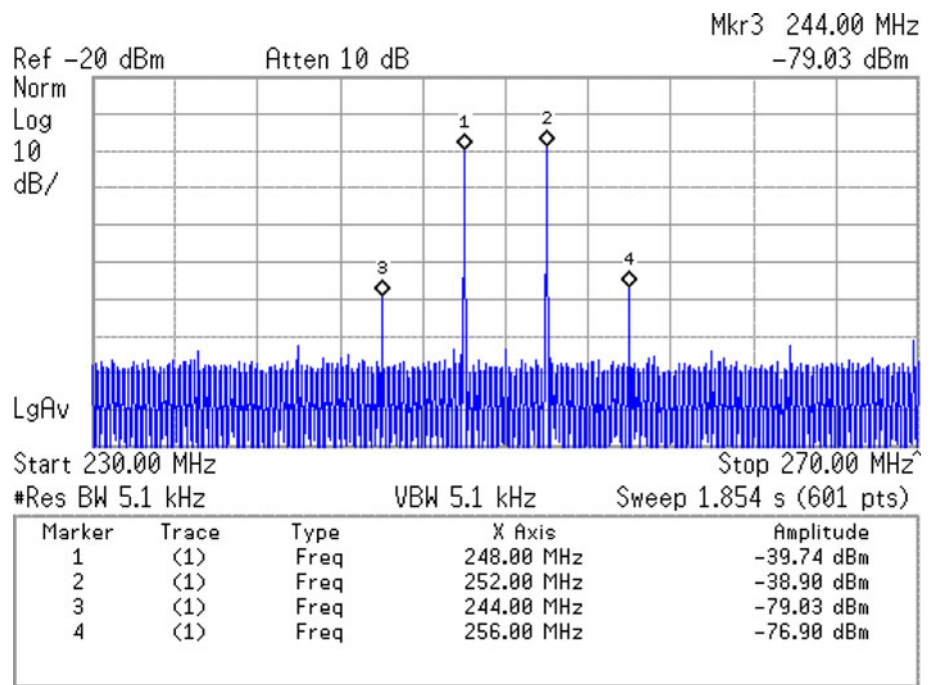


Table 1 Comparison of previously reported works

Reference	[11]	[12]	[13]	This work
	ESSCIRC 2006	A-SSCC 2006	ISSCC 2007	
Technology	0.12- μ m CMOS	0.18- μ m CMOS	0.13- μ m CMOS	0.18- μ m CMOS
Filter order	3	8	5	4
-3 dB frequency (MHz)	235	250	240	250
IM ³ /HD3	-43 dB HD3 @ 50 MHz	-37 dB HD3 @ 150 MHz	-	-40 dB IM3 @ 250 MHz
IIP3	-	-	- 4.82 dBV	3 dBV
Supply voltage	1.5	1.8	1.2	1

^a Usually IM3 shows the worst case condition to the measurement

Acknowledgments The authors would like to thank the National Chip Implementation Center of Taiwan for supporting the chip fabrication.

References

1. Lo, T. Y., Hung, C. C., & Ismail, M. (2007). A wide tuning range G_m -C filter for multi-mode direct-conversion wireless receivers. In *Proc. Eur. Solid-State Circuits Conf.* (pp. 210–213). Sep 2007.
2. Lo, T. Y., & Hung, C. C. (2007). Low-voltage multi-mode G_m -C channel selection filter for mobile applications. In *IEEE Custom Integrated Circuit Conference* (pp. 635–638). Sep 2007.

3. Hung, C. C., Halonen, K., Ismail, M., Porra, V., & Hyogo, A. (1997). A low-voltage, low-power CMOS fifth-order elliptic G_m -C filter for baseband mobile, wireless communication. *IEEE Transactions on Circuits and Systems for Video Technology*, 7, 584–593.
4. Yodprasit, U., & Enz, C. C. (2003). A 1.5-V 75-dB dynamic range third-order G_m -C filter integrated in a 0.18- μ m standard digital CMOS process. *IEEE Journal of Solid-State Circuits*, 38(7), 1189–1197.
5. Mourabit, A. E., Lu, G.-N., & Pittet, P. (2005). Wide-linear-range subthreshold OTA for low-power, low-voltage, and low-frequency applications. *IEEE Transactions on Circuits and Systems I: Regular Papers*, 52(8), 1481–1488.
6. Rodriguez-Villegas, E., Yufera, A., & Rueda, A. (2004). A 1.25-V micropower G_m -C filter based on FG MOS transistors operating in weak inversion. *IEEE Journal of Solid-State Circuits*, 39(1), 100–111.
7. Chen, M., Silva-Martínez, J., Rokhsaz, S., & Robinson, M. (2003). A 2- V_{pp} 80–200-MHz fourth-order continuous-time linear phase filter with automatic frequency tuning. *IEEE Journal of Solid-State Circuits*, 38(10), 1745–1749.
8. Rezzi, F., Baschiroto, A., & Castello, R. (1995). A 3 V 12–55 MHz BiCMOS pseudo-differential continuous-time filter. *IEEE Transactions on Circuits and Systems I*, 42(11), 896–903.
9. Nader Mohieldin, A., Sánchez-Sinencio, E., & Silva-Martínez, J. (2003). A fully balanced pseudo-differential OTA with common-mode feedforward and inherent common-mode feedback detector. *IEEE Journal of Solid-State Circuits*, 38(4), 663–668.
10. Silva-Martínez, J., Adut, J., Rocha-Perez, J., Robinson, M., & Rokhsaz, S. (2003). A 60 mW, 200 MHz continuous-time seventh-order linear phase filter with on-chip automatic tuning system. *IEEE Journal of Solid-State Circuits*, 38, 216–225.
11. Kolm, R., & Zimmermann, H. (2006). A 3rd-order 235 MHz low-pass gmC-filter in 120 nm CMOS. In *Proc. Eur. Solid-State Circuits Conf.* (pp. 215–218).
12. Lee, C. C., & Yang, T. Y. (2006). A tuning technique for bandwidth of programmable gain filter. In *IEEE A-SSCC Dig. Tech. Papers* (pp. 175–178).

13. Sarri, V., Kaltiokallio, M., Lindfors, S., Ryyänen, J., & Halonen, K. (2007). A 1.2 V 240 MHz CMOS continuous-time low-pass filter for a UWB radio receiver. In *IEEE ISSCC Dig. Tech. Papers* (pp. 122–123).



Tien-Yu Lo received the BS, MS, and PhD degrees in communication engineering from National Chiao Tung University, Hsinchu, Taiwan, in 2001, 2003, and 2007, respectively. Since 2008, he has been with MediaTek Inc., as an analog IC designer. His research interests include low-voltage analog and mixed-signal integrated circuits.



Chung-Chih Hung was born in Tainan, Taiwan. He received the BS degree in electrical engineering from National Taiwan University, Taipei, Taiwan, in 1989, and the MS and PhD degrees in electrical engineering from The Ohio State University, Columbus, Ohio, in 1993 and 1997, respectively. From 1989 to 1991, he served in the Taiwan Marine Corps as a communication officer. From 1997 to 2003, he worked for several IC design companies in San Jose, CA, and

San Diego, CA, where he held analog circuit design manager and

director positions. Since 2003, he has been with National Chiao Tung University, Hsinchu, Taiwan, where he is currently an Associate Professor in the Department of Electrical Engineering. His research interests include the design of analog and mixed-signal integrated circuits for communication and high-speed applications.